Supplemental Material

Porphyromonas gingivalis suppresses oral squamous cell carcinoma progression by inhibiting MUC1 and remodeling tumor microenvironment

Fig. S1

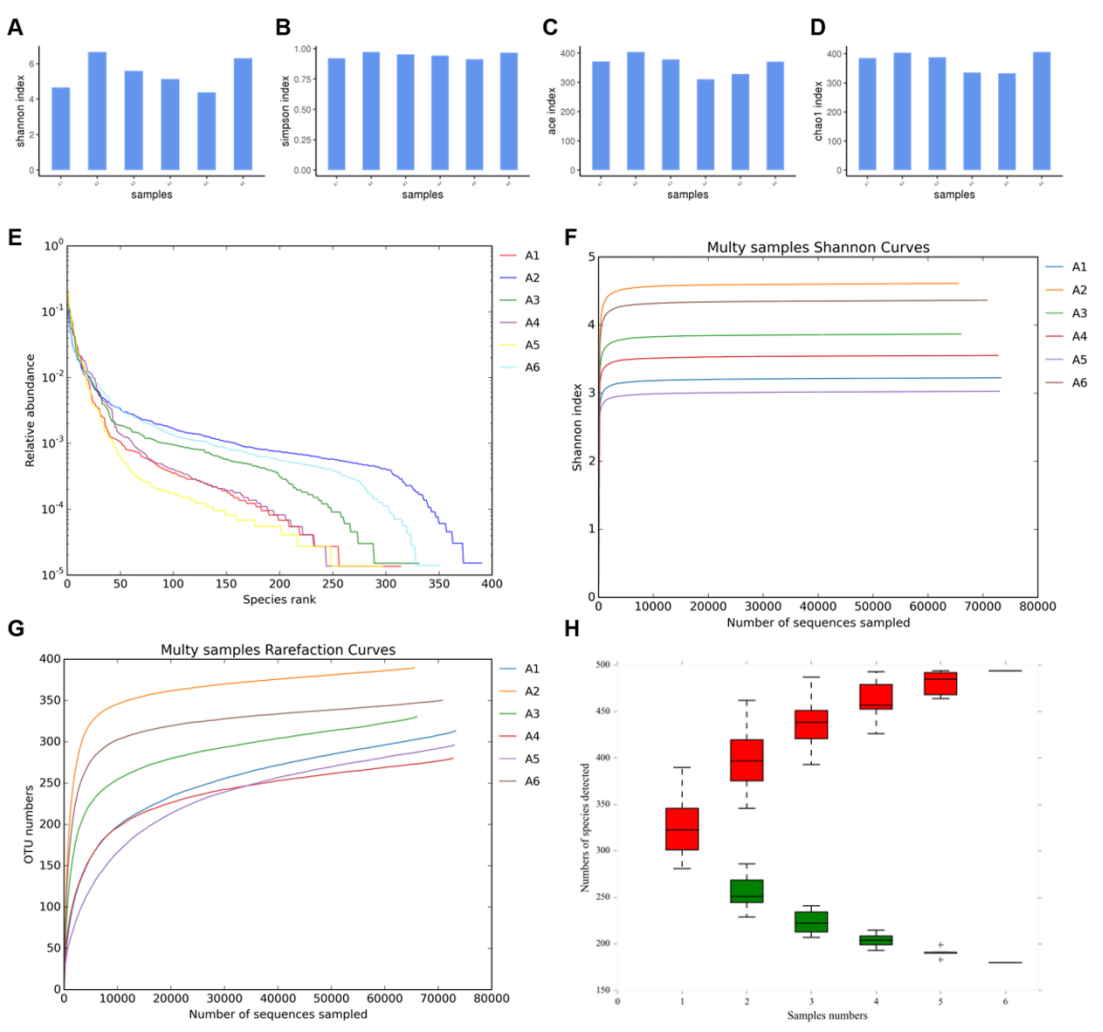

Fig. S1. Alpha diversity of microbiomes in OSCC tissues. A) Shannon and B) Simpson indices were used to demonstrate species diversity, the C) Ace indices and D) chao1 indices reflected species richness. E) Rank abundance curve. F) Shannon exponential curve, G) Rarefaction Curve and H) cumulative relative abundance curve of OSCC samples.

Fig. S2

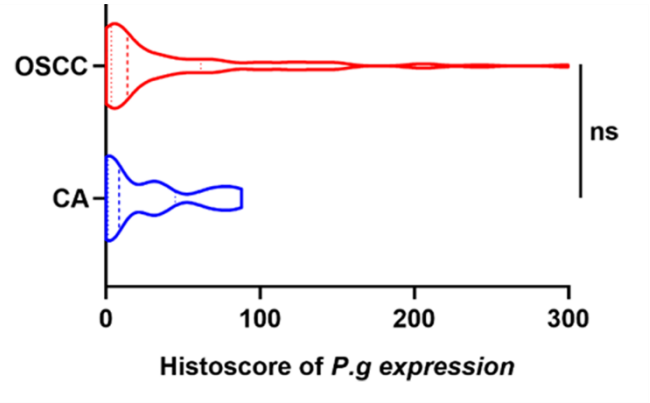

Fig. S2 The IHC analysis of *P.gingivalis* expression per μm^2 in OSCC and CA. CA, Adjacent cancer. The data are represented as Mean±SD, CA=23, OSCC=56 (Mann-Whitney test was used. ns, not significant, scale bar=100μm).

Fig. S3

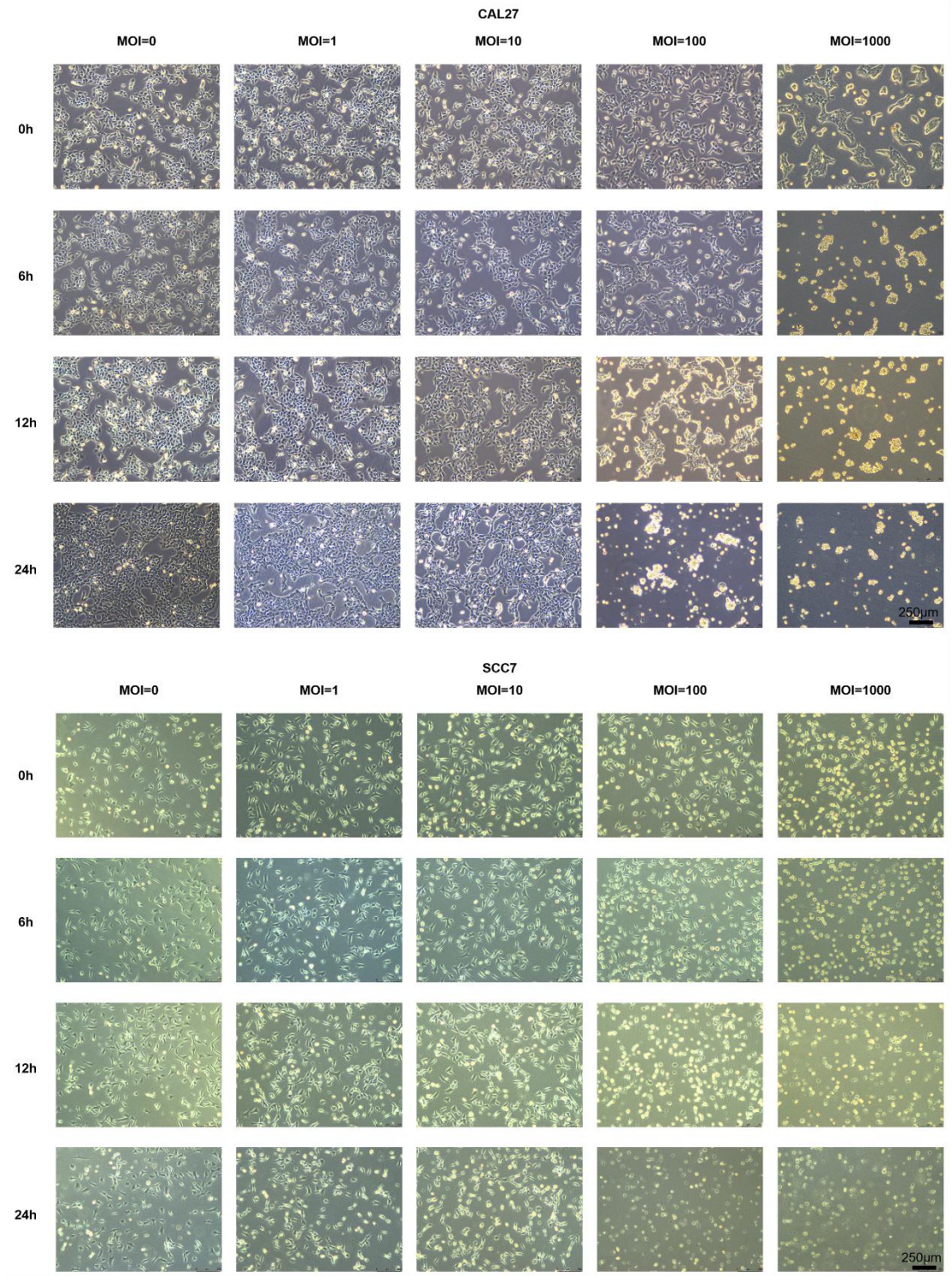

Fig. S3. CAL27 and SCC7 treated with *P. gingivalis* at different concentrations and times under microscope. Scale bar = 250 μm. All experiments were independently repeated in triplicate.

Fig. S4

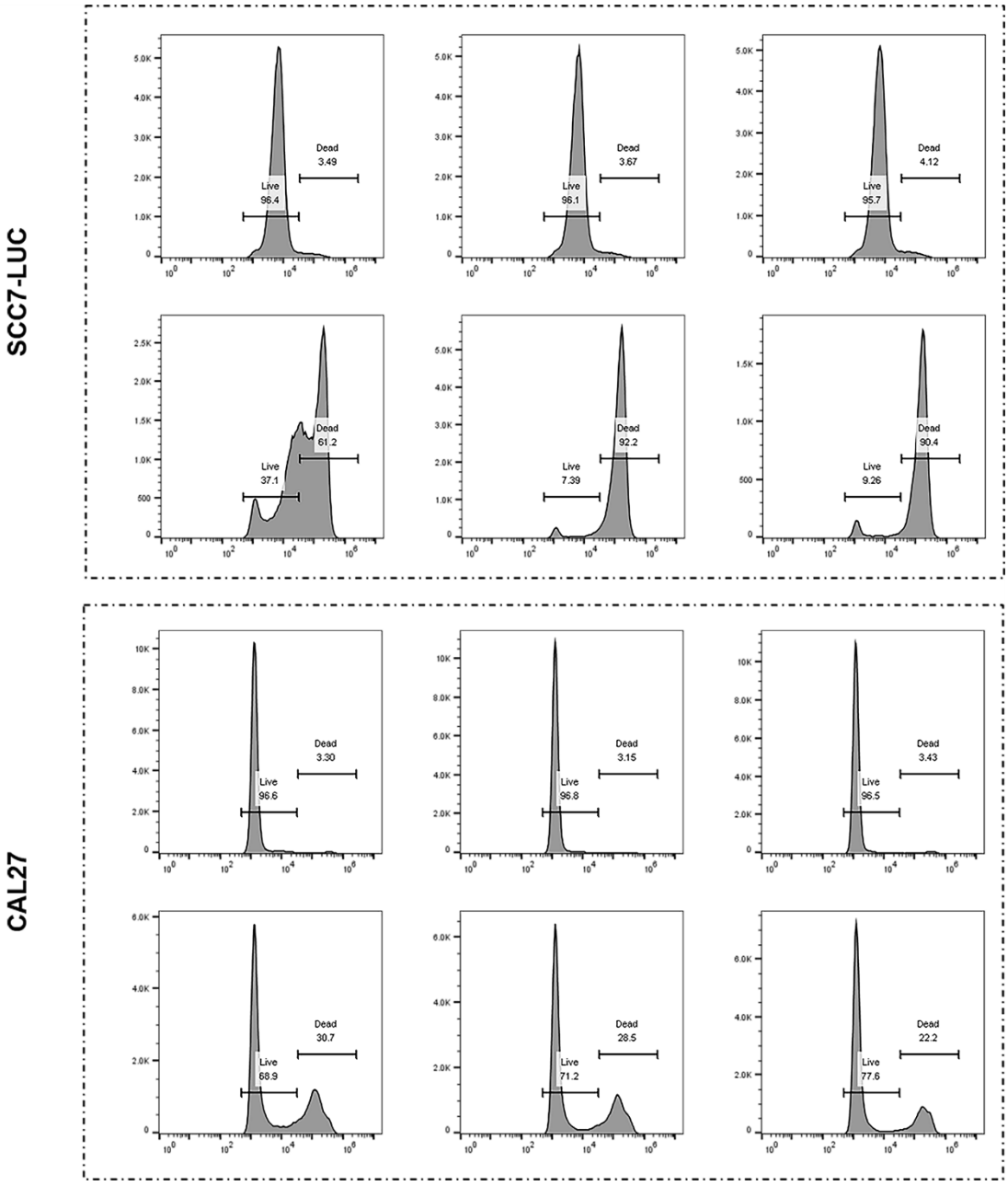

Fig. S4. Flow cytometry analysis of the death ratio of CAL27 and SCC7 disposed with or without *P. gingivalis* (MOI = 1000) for 24 hours. All experiments were independently repeated in triplicate.

Fig. S5

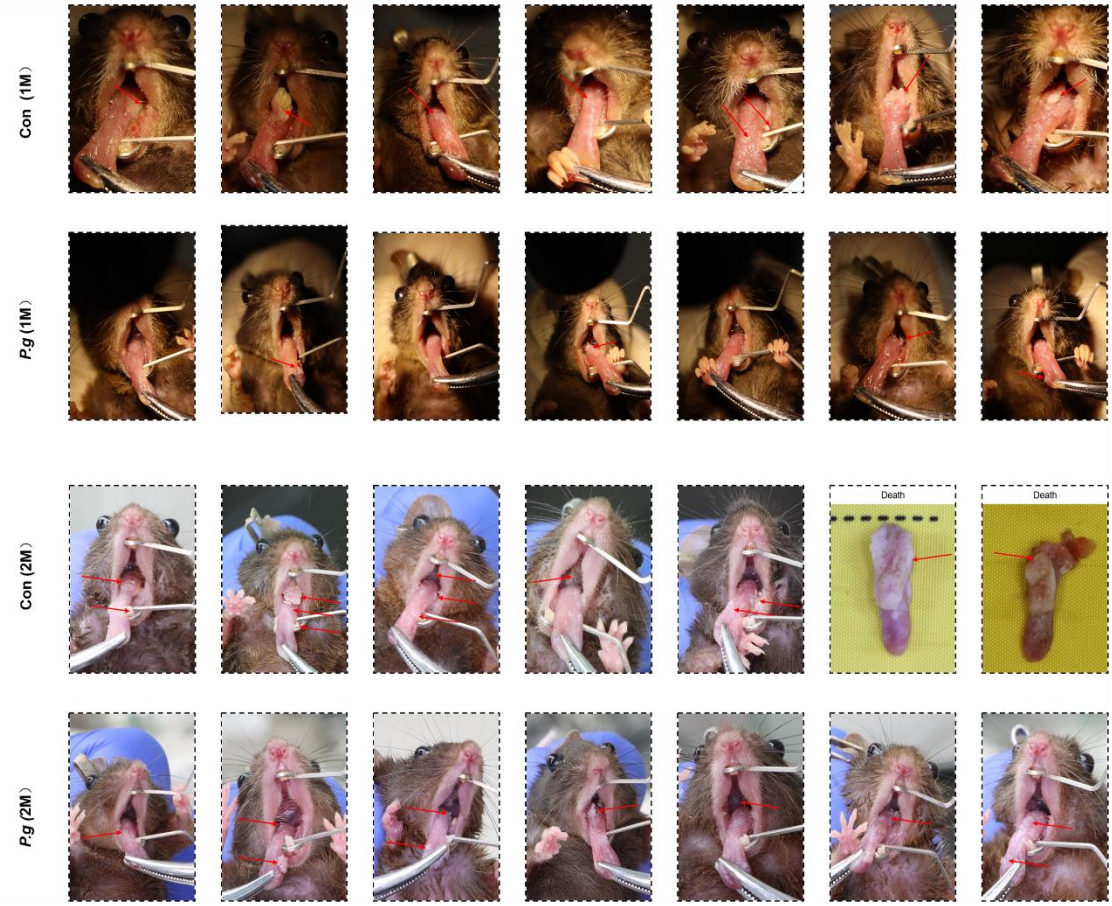

Fig. S5. Real-time monitoring tumors of 4NQO mice disposed with or without *P. gingivalis* for one month and two months (n=7).

Fig S6

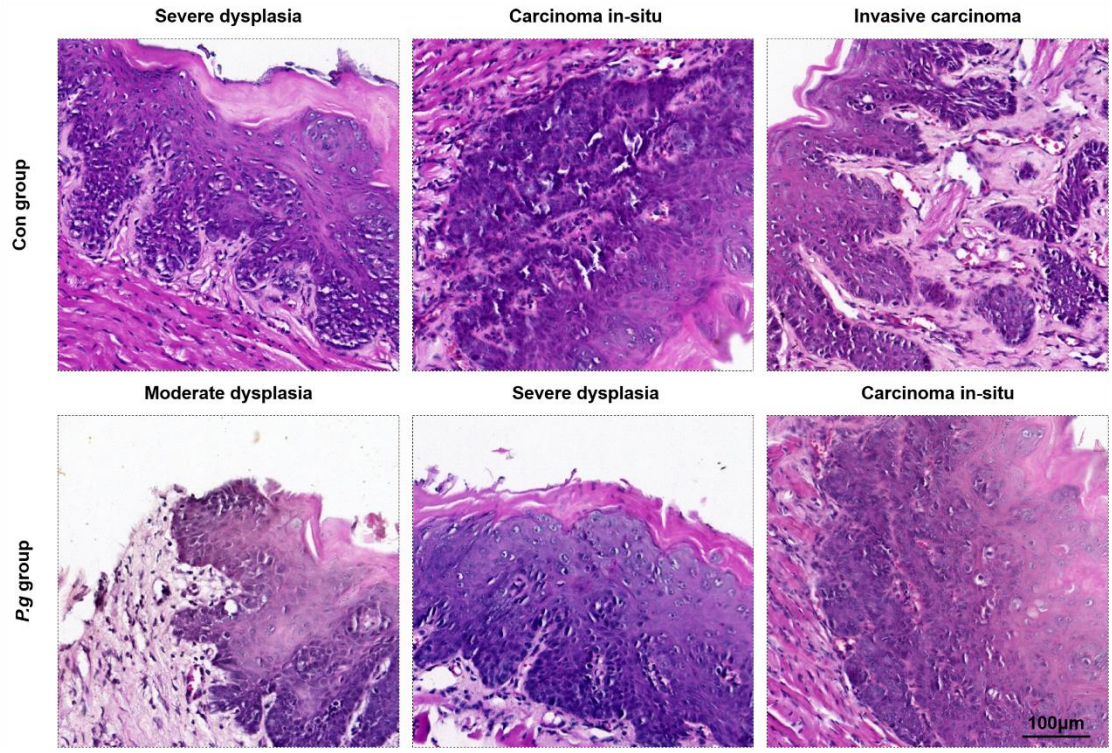

Fig. S6 Representative pictures of HE staining, containing mild to severe dysplasia, carcinoma in situ and invasive carcinoma. (n=5, Scale Bar=100μm).

Fig. S7

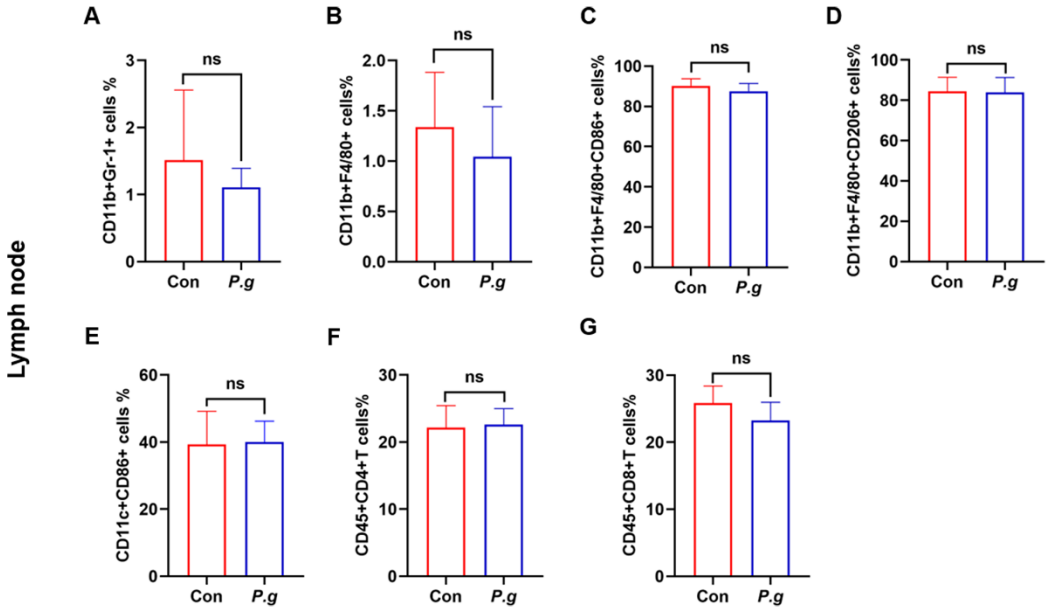

Fig. S7. Various infiltrating immune cell subsets in the lymph nodes of 4NQO-induced mice. The percentage of tumor-infiltrating **A.** $CD11b^+$ $Gr\text{-}1^+$ MDSCs, **B.** $CD11b^+$ $F4/80^+$ Macrophages, **C.** $CD11b^+$ $F4/80^+$ $CD86^+$ M1-like Macrophages, **D.** $CD11b^+$ $F4/80^+$ $CD206^+$ M2-like Macrophages, **E.** $CD11c^+$ $CD86^+$ Matured DCs, **F.** $CD4^+$ T cells and **G.** $CD8^+$ T cells were compared. All data are represented as Mean±SD, n=3. (Unpaired t test Welch's correction was used for MDSC, unpaired t test was used for the rest, ns, not significant).

Fig. S8

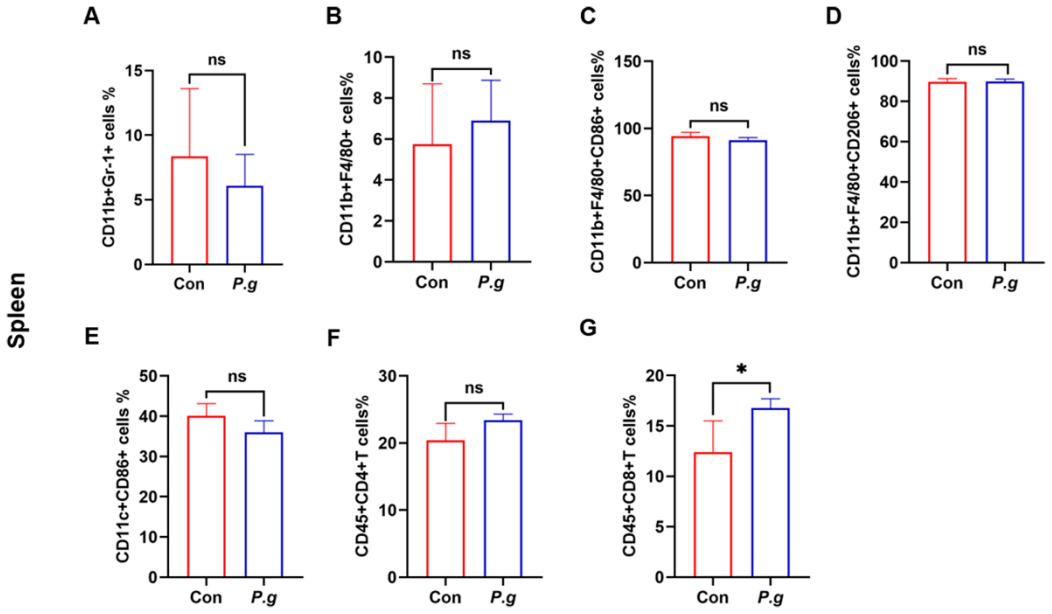

Fig. S8. Various infiltrating immune cell subsets in the spleen of 4NQO-induced mice. The percentage of tumor-infiltrating **A.** $CD11b^+$ $Gr\text{-}1^+$ MDSCs, **B.** $CD11b^+$ $F4/80^+$ Macrophages, **C.** $CD11b^+$ $F4/80^+$ $CD86^+$ M1-like Macrophages, **D.** $CD11b^+$ $F4/80^+$ $CD206^+$ M2-like Macrophages, **E.** $CD11c^+$ $CD86^+$ Matured DCs, **F.** $CD4^+$ T cells and **G.** $CD8^+$ T cells were compared. All data are represented as Mean±SD, n=3. (Unpaired t test with Welch's correction was used for $CD8^+$T cells, unpaired t test was used for the rest, *, $P < 0.05$; ns, not significant).